A "click-based" porous organic polymer from tetrahedral building blocks†

Prativa Pandey,‡ Omar K. Farha,‡ Alexander M. Spokoyny, Chad A. Mirkin, Mercouri G. Kanatzidis, Joseph T. Hupp and SonBinh T. Nguyen*

Received 15th October 2010, Accepted 12th November 2010
DOI: 10.1039/c0jm03483e

A thermally and chemically stable "click-based" porous organic polymer with high surface area was synthesized from two tetrahedral building blocks.

Highly crosslinked, microporous organic polymers[1–7] have recently received significant attention as potential materials for a variety of applications ranging from gas storage[8–10] and gas separation,[11,12] to chemical catalysis,[13] chemical sensing,[14] and capture of improvised chemical threats such as ammonia.[15] Depending on the design, synthetic strategy, and properties, these materials have been classified into several subsets including amorphous hyper-crosslinked polymers (HCPs),[16,17] polymers of intrinsic microporosity (PIMs),[12,18] conjugated microporous polymers (CMPs),[19] porous organic polymers (POPs),[11,20] porous organic frameworks (POFs),[21] and (crystalline) covalent organic frameworks (COFs).[1] Regardless of the degree of crystallinity, the pore properties of these materials can often be modulated based on the choice of the building blocks. Notably, organic materials with high surface areas can be made from all-planar building blocks[2,21] as well as from combinations of non-planar "struts".[1,11] Herein, we report the synthesis of a highly stable, microporous "click-based" porous organic polymer (POP) *via* copper-catalyzed alkyne–azide coupling (CuAAC) between two rigid tetrahedral building blocks (T_d + T_d).[22]

Alkyne–azide "click" chemistry has been widely employed in the syntheses of both linear and crosslinked polymers with diverse applications ranging from drug delivery[23–25] to electronics.[26,27] Our groups have applied this strategy in the modification of porous materials such as MOFs[28,29] and nanobins.[30] Given the aromatic, rigid nature of the 1,2,3-triazole group that results from alkyne–azide coupling, we reasoned that highly crosslinked organic polymers synthesized using this strategy would possess permanent microporosity and be attractive materials for gas storage. In addition, the high stability of the 1,2,3-triazole linkage could give "click-based" POPs thermal- and chemical-stability advantages over other polymers obtained *via* alternative bond-construction strategies.

The CuAAC reaction between tetrakis(4-ethynylphenyl)methane (**C1**) and tetrakis(4-azidophenyl)methane (**D1**) (Scheme 1) occurs readily in dimethylformamide (DMF) at both room temperature and 100 °C to give several versions of POP **C1–D1** as brown powders. Since the surface area of the POP synthesized at 100 °C (1260 $m^2 g^{-1}$) was much higher than that for the version synthesized at 25 °C

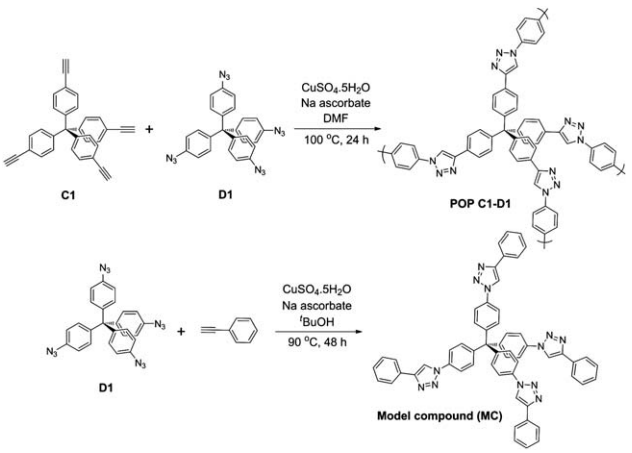

Scheme 1 Top: synthesis of "click-based" POP **C1–D1** from monomers **C1** and **D1** using copper-catalyzed alkyne–azide coupling. Bottom: synthesis of model compound (tetrakis(4-(4-phenyl-1*H*-1,2,3-triazol-1-yl)-phenyl)methane; **MC**).

(440 $m^2 g^{-1}$), further optimization of the synthesis was carried out at the higher temperature (Table S1, entries 3 and 6 and Fig. S2 in the ESI†). The yield for POP **C1–D1** (Table 1, entry 1a) was almost quantitative, suggesting that crosslinking was nearly complete with no soluble oligomers. However, care must be taken in isolating the product as a fraction in fine particulates can be lost if the filtration is carried out over filter paper (Table 1, entries 1b–5, see also Table S1 entries 1b–6 in the ESI†). Loss of this component during the filtration process can result in a slight decrease of the specific surface area of the overall product (1360 $m^2 g^{-1}$ *vs.* 1440 $m^2 g^{-1}$, Table 1 *cf.* entries 1a and 1b) but does not significantly affect the micropore and total pore volumes.

Because the progress of CuAAC depends on the availability of Cu^I intermediates, which in turn depends on the amount of sodium ascorbate reducing agent, we optimized the porosity of the product POP **C1–D1** by adjusting the amount of sodium ascorbate between 10 and 70 mol%, while keeping the amount of copper catalyst constant (10 mol%). Surprisingly, the surface area of POPs **C1–D1** systematically decreased with increasing amount of sodium ascorbate in the reaction mixture (Table 1 and Fig. S1 in the ESI†). Treatment of these POPs *via* Soxhlet extraction (to remove any sodium ascorbate possibly present in the pores) did not result in improvement in the original surface areas (Table S2 in the ESI†). Thus, we attribute the aforementioned ascorbate-induced lowering of surface area to an increase in catalyst availability: at higher loadings of ascorbate more Cu^I is available, allowing for more crosslinking to occur within the porous network and thus lowering surface areas. This hypothesis is supported by a progressive decrease in micropore volume and total pore volume as the amount of ascorbate is increased.

Department of Chemistry and the International Institute for Nanotechnology, Northwestern University, 2145 Sheridan Road, Evanston, IL, 60208-3113, USA. E-mail: stn@northwestern.edu

† Electronic supplementary information (ESI) available: Detailed experimental procedures, materials, instrumentation, and characterization. DOI: 10.1039/c0jm03483e

‡ These authors contributed equally to this work.

Table 1 Surface-area and pore properties of "click" POP **C1–D1** synthesized by varying the amount of sodium ascorbate

Entry[a]	Sodium ascorbate (mol%)	Specific surface area ($m^2\ g^{-1}$)	Micropore volume ($cm^3\ g^{-1}$)	Total pore volume ($cm^3\ g^{-1}$)	Yield (%)
1a[b]	10	1440	0.56	0.76	>99
1b[c]	10	1360	0.53	0.74	67
2[c]	20	1320	0.51	0.73	62
3[c]	30	1260	0.49	0.67	64
4[c]	50	1140	0.44	0.64	81
5[c]	70	1090	0.42	0.52	77

[a] All reactions were carried out in DMF at 100 °C using 10 mol% $CuSO_4 \cdot 5H_2O$ and at 0.04 M solution of azide functional group (1 : 1 alkyne-to-azide functional group ratio). [b] Obtained using workup procedure II. [c] Obtained using workup procedure I.

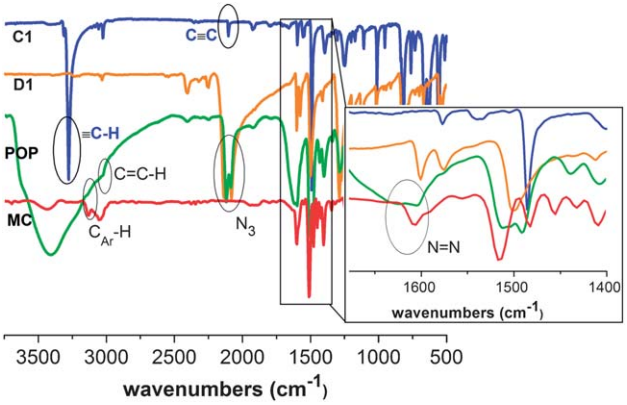

Fig. 1 FTIR spectra of the starting materials (**C1** and **D1**), POP **C1–D1** (Table 1, entry 1b), and model compound (**MC**).

The FTIR spectrum of POP **C1–D1** (Table 1, entry 1b) compares well with that of a model compound (**MC**, Scheme 1). A broad N=N stretch can be observed at 1610 cm^{-1} (Fig. 1), together with a weak C=CH band at 3029 cm^{-1}, consistent with the formation of the expected triazole ring. However, IR stretches from unreacted azide could still be observed at 2114 cm^{-1}, suggesting that the azide–alkyne coupling is incomplete. Interestingly, a strong and broad stretch at ~3300 cm^{-1} is also observed, suggesting the presence of significant amounts of physisorbed water. The solid state ^{13}C CPMAS NMR spectrum of POP **C1–D1** (Table 1, entry 1b) matches well with that of **MC**, further supporting the formation of cyclic triazole linkages (Fig. 2).

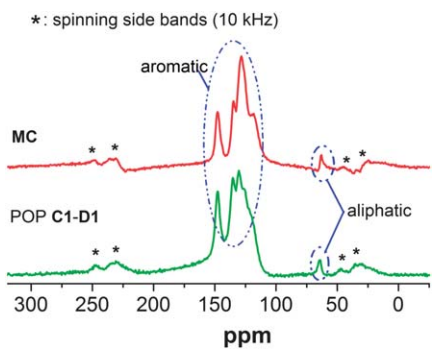

Fig. 2 ^{13}C CPMAS NMR spectra of the model compound (**MC**) and POP **C1–D1** (Table 1, entry 1b).

Thermogravimetric analysis (TGA) of dried POP **C1–D1** shows that this microporous material is thermally stable, losing only 20 wt% of its mass below 500 °C (Fig. S8 in the ESI†). The thermal stability of this uncapped material approaches those of the most stable metal-organic framework analogues containing carborane[31–33] or Zr building blocks.[34] The powder X-ray diffraction spectrum of POP **C1–D1** is featureless, implying (as expected) that it is amorphous.

Consistent with the anticipated chemical stability of the 1,2,3-triazole linkage,[35] POP **C1–D1** is remarkably stable. Immersing **C1–D1** in 6 N NaOH (aq) or 6 N HCl (aq) at 60 °C for 8 h leads to essentially no change in internal surface area (Table S3 in the ESI†). Increasing the immersion temperature to 80 °C and time to 24 h leads to only slight decreases (10–12%) in surface area (Table S3 in the ESI†). This acid- and base- stability rivals that of zeolitic imidazolate frameworks[36] and greatly exceeds that of imine-linked POPs having comparable initial surface areas;[21] the surface areas of the latter rapidly decrease following exposure to water. Its chemical stability is also superior to those of diimide-linked POPs,[11,20] which are stable in relatively dilute aqueous acids (0.1 N) but not in bases.

High uptake of nitrogen at low pressure, as observed in the N_2 adsorption–desorption isotherms for the various preparations of POP **C1–D1** (Fig. 3, see also Fig. S1 in the ESI†), suggests that these materials are mainly microporous. However, the isotherms of POPs prepared with smaller amounts of sodium ascorbate (10–30 mol%) tend to exhibit more hysteresis than those prepared with larger amounts (50–70 mol%). The slopes of the isotherm adsorption branches for the latter materials are also less steep than those for the former. Particularly interesting is the presence of a pronounced

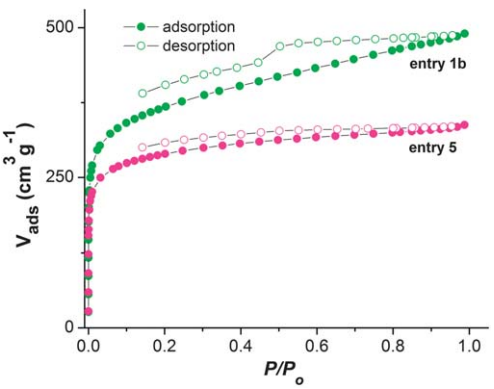

Fig. 3 N_2 adsorption–desorption isotherms at 77 K for two versions of POP **C1–D1** (Table 1, entries 1b and 5). A complete set of isotherms for all samples can be found in Fig. S1 in the ESI†.

hysteretic step in the N_2 isotherm desorption branch for the POPs prepared with low amounts (10–30 mol%, Table 1, entries 1a–3) of sodium ascorbate (Fig. 3, see also Fig. S1 in the ESI†). In contrast, there is no hysteretic step in the N_2 isotherm desorption branch for the POPs prepared by using higher amounts (50–70 mol%, Table 1, entries 4 and 5) of sodium ascorbate (Fig. 3, see also Fig. S1 in the ESI†).

For the samples of POP **C1–D1** whose isotherms contain no hysteretic desorption step (Fig. 3 and Table 1, entries 4 and 5), the parallel, almost-horizontal nature of the two branches of the isotherm implies the presence of only narrow slit-like pores.[37,38] In contrast, the samples whose isotherms contain a hysteretic desorption step (Fig. 3 and Table 1, entries 1a–3) likely possess more complex pore geometry.[37,38] The near-horizontal desorption behavior in the $0.5 < P/P_o < 1$ region and the abrupt switch into a slightly steeper desorption behavior in the $P/P_o < 0.5$ region (for N_2 adsorption at 77 K, this switch often occurs near the $P/P_o = 0.42$ point[37]) indicate that the pores are not all slit-like. The upward-sloping trend in the adsorption branch of these isotherms, which becomes steeper at higher pressures, has been attributed by others to the presence of pores of different shapes and sizes (mainly microporous with some higher micropores and lower mesopores).[37]

Despite the aforementioned indications of complex pore geometry, non-local density functional theory (NLDFT) pore size distribution analysis of POP **C1–D1** prepared using 10 mol% sodium ascorbate (Table 1, entry 1b) indicates a mainly microporous material with a narrow pore-size distribution centered around a primary pore width of 9.2 Å (Fig. 4). This width is much smaller than expected (~21 Å) for an idealized diamond-like single network formed by simply "clicking" together monomers **C1** and **D1**. This disparity constitutes strong evidence for interpenetration in the hyper-crosslinked networks constituting POP **C1–D1**.

Given the high surface area and narrow pore-size distribution of POP **C1–D1**, we explored its potential to adsorb the gases CO_2 and H_2. The NLDFT surface area obtained for POP **C1–D1** (Table 1, entry 1a and Fig. S7 in the ESI†) based upon adsorption of CO_2 at 273 K is 1080 $m^2\ g^{-1}$. This POP has a reasonably good H_2 adsorption capacity at 77 K and 1 bar (1.6 wt%, Fig. 5a), comparable to a range of MOFs,[39] carbon materials,[8,40] and microporous polymers[10,41] featuring similar or higher surface areas. The isosteric heat of hydrogen adsorption for this material, which is an approximate measure of the strength of its interaction with H_2, was found to be 7.9 kJ mol^{-1} at low surface coverage, decreasing to 4.0 kJ mol^{-1} at 1 bar (Fig. 5b). These values are typical for H_2 adsorption in micropores of materials that can offer only London dispersion-type interactions.

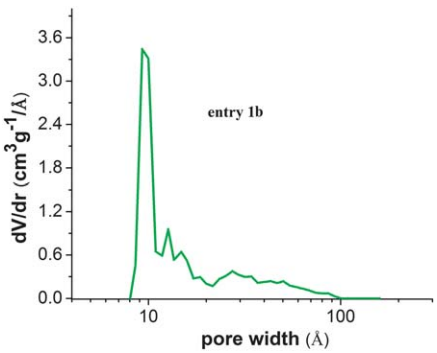

Fig. 4 Pore size distribution plot for POP **C1–D1** (Table 1, entry 1b) according to NLDFT analysis.

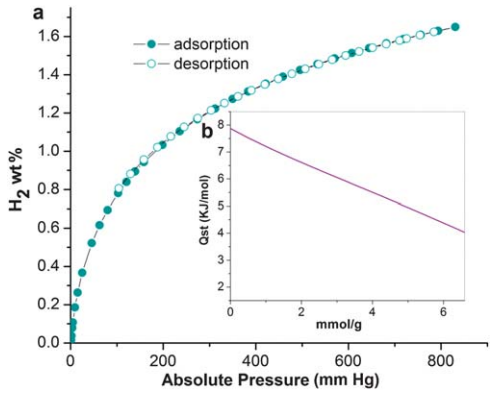

Fig. 5 (a) H_2 adsorption–desorption isotherm for POP **C1–D1** (Table 1, entry 1a) at 77 K, up to *ca.* 1 bar. (b) Isosteric heat of H_2 adsorption of POP **C1–D1** (Table 1, entry 1a). Measurements were carried out at 77 K and 87 K.

In summary, we have shown that a permanently microporous POP can be assembled readily from a complementary pair of tetrahedral building blocks (T_d + T_d) using CuAAC chemistry. The resulting material is thermally stable, as well as chemically stable, easily surviving exposure to highly acidic and basic solutions. The excellent stability of POP **C1–D1** suggests more generally that cyclic-triazole-linked POP materials can serve as excellent engineering materials under a wide range of conditions. At 1 bar, the micropores of this material have reasonably good ambient-temperature adsorption of CO_2 and cryogenic adsorption of H_2. We are actively exploring structure–property relationships for these types of materials and efforts to turn them into high-surface-area and morphologically well-defined nano- and microparticle structures, similar to infinite coordination polymer particle analogues.[42–46] Such capabilities will allow researchers to tune the properties of this novel class of materials for optimal performance in many practical applications, including gas storage, catalysis, and biological probe design.

We gratefully acknowledge the US DOE-EERE (Grant No. DE-FG36-08GO18137/A001), DTRA, AFOSR, and the NSF-NSEC for financial support. Instruments in the Northwestern University Integrated Molecular Structure Education and Research Center (IMSERC) were purchased with grants from NSF-NSEC, NSF-MRSEC, the Keck Foundation, the state of Illinois, and Northwestern University. We thank Dr Alexandros P. Katsoulidis for helpful discussions.

Notes and references

1 F. J. Uribe-Romo, J. R. Hunt, H. Furukawa, C. Klöck, M. O'Keeffe and O. M. Yaghi, *J. Am. Chem. Soc.*, 2009, **131**, 4570–4571.
2 M. G. Schwab, B. Fassbender, H. W. Spiess, A. Thomas, X. Feng and K. Müllen, *J. Am. Chem. Soc.*, 2009, **131**, 7216–7217.
3 T. Tozawa, J. T. A. Jones, S. I. Swamy, S. Jiang, D. J. Adams, S. Shakespeare, R. Clowes, D. Bradshaw, T. Hasell, S. Y. Chong, C. Tang, S. Thompson, J. Parker, A. Trewin, J. Bacsa, A. M. Z. Slawin, A. Steiner and A. I. Cooper, *Nat. Mater.*, 2009, **8**, 973–978.
4 H. M. El-Kaderi, J. R. Hunt, J. L. Mendoza-Cortes, A. P. Côte, R. E. Taylor, M. O'Keeffe and O. M. Yaghi, *Science*, 2007, **316**, 268–272.

5 A. P. Côte, A. I. Benin, N. W. Ockwig, M. O'Keeffe, A. J. Matzger and O. M. Yaghi, *Science*, 2005, **310**, 1166–1170.
6 N. B. McKeown and P. M. Budd, *Macromolecules*, 2010, **43**, 5163–5176.
7 J. Germain, F. Svec and J. M. J. Fréchet, *Chem. Mater.*, 2008, **20**, 7069–7076.
8 A. Thomas, P. Kuhn, J. Weber, M.-M. Titirici and M. Antonietti, *Macromol. Rapid Commun.*, 2009, **30**, 221–236.
9 T. Ben, H. Ren, S. Ma, D. Cao, J. Lan, X. Jing, W. Wang, J. Xu, F. Deng, J. Simmons, S. Qiu and G. Zhu, *Angew. Chem., Int. Ed.*, 2009, **48**, 9457–9460.
10 J. Weber and A. Thomas, *J. Am. Chem. Soc.*, 2008, **130**, 6334–6335.
11 O. K. Farha, A. Spokoyny, B. Hauser, Y.-S. Bae, S. Brown, R. Q. Snurr, C. A. Mirkin and J. T. Hupp, *Chem. Mater.*, 2009, **21**, 3033–3035.
12 N. B. McKeown and P. M. Budd, *Chem. Soc. Rev.*, 2006, **35**, 675–683.
13 H. J. Mackintosh, P. M. Budd and N. B. McKeown, *J. Mater. Chem.*, 2008, **18**, 573–578.
14 N. A. Rakow, M. S. Wendland, J. E. Trend, R. J. Poirier, D. M. Paolucci, S. P. Maki, C. S. Lyons and M. J. Swierczek, *Langmuir*, 2010, **26**, 3767–3770.
15 C. J. Doonan, D. J. Tranchemontagne, T. G. Glover, J. R. Hunt and O. M. Yaghi, *Nat. Chem.*, 2010, **2**, 235–238.
16 M. P. Tsyurupa and V. A. Davankov, *React. Funct. Polym.*, 2006, **66**, 768–779.
17 M. P. Baya, P. A. Siskos and V. A. Davankov, *J. AOAC Int.*, 2000, **83**, 579–583.
18 P. M. Budd, B. S. Ghanem, S. Makhseed, N. B. McKeown, K. J. Msayib and C. E. Tattershall, *Chem. Commun.*, 2004, 230–231.
19 J.-X. Jiang, F. Su, H. Niu, C. D. Wood, N. L. Campbell, Y. Z. Khimyak and A. I. Cooper, *Chem. Commun.*, 2008, 486–488.
20 O. K. Farha, Y.-S. Bae, B. G. Hauser, A. M. Spokoyny, R. Q. Snurr, C. A. Mirkin and J. T. Hupp, *Chem. Commun.*, 2010, **46**, 1056–1058.
21 P. Pandey, A. P. Katsoulidis, I. Eryazici, Y. Wu, M. G. Kanatzidis and S. T. Nguyen, *Chem. Mater.*, 2010, **22**, 4974–4979.
22 While we were completing experimental work on the current manuscript, a paper by Holst *et al.* (J. R. Holst, E. Stöckel, D. J. Adams and A. I. Cooper, *Macromolecules*, 2010, **43**, 8531–8538) appeared on the use of tetrahedral monomers to create conjugated microporous polymers (CMPs) *via* a wide range of strategies, one of which was "click" chemistry. As the manuscript by Holst *et al.* was focused primarily on CMPs derived from metal-catalyzed coupling, the synthesis and properties of the click-derived network were only very briefly described.
23 M. J. Joralemon, R. K. O'Reilly, C. J. Hawker and K. L. Wooley, *J. Am. Chem. Soc.*, 2005, **127**, 16892–16899.
24 W. H. Binder and R. Sachsenhofer, *Macromol. Rapid Commun.*, 2007, **28**, 15–54.
25 P. Wu, M. Malkoch, J. N. Hunt, R. Vestberg, E. Kaltgrad, M. G. Finn, V. V. Fokin, K. B. Sharpless and C. J. Hawker, *Chem. Commun.*, 2005, 5775–5777.
26 A. Qin, J. W. Y. Lam and B. Z. Tang, *Chem. Soc. Rev.*, 2010, **39**, 2522–2544.
27 X. Chen, A. Braunschweig, M. Wiester, S. Yeganeh, M. Ratner and C. Mirkin, *Angew. Chem., Int. Ed.*, 2009, **48**, 5178–5181.
28 T. Gadzikwa, G. Lu, C. L. Stern, S. R. Wilson, J. T. Hupp and S. T. Nguyen, *Chem. Commun.*, 2008, 5493–5495.
29 T. Gadzikwa, O. K. Farha, C. D. Malliakas, M. G. Kanatzidis, J. T. Hupp and S. T. Nguyen, *J. Am. Chem. Soc.*, 2009, **131**, 13613–13615.
30 S.-M. Lee, H. Chen, T. V. O'Halloran and S. T. Nguyen, *J. Am. Chem. Soc.*, 2009, **131**, 9311–9320.
31 O. K. Farha, A. M. Spokoyny, K. L. Mulfort, M. F. Hawthorne, C. A. Mirkin and J. T. Hupp, *J. Am. Chem. Soc.*, 2007, **129**, 12680–12681.
32 O. K. Farha, A. M. Spokoyny, K. L. Mulfort, S. Galli, J. T. Hupp and C. A. Mirkin, *Small*, 2009, **5**, 1727–1731.
33 Y.-S. Bae, O. K. Farha, A. M. Spokoyny, C. A. Mirkin, J. T. Hupp and R. Q. Snurr, *Chem. Commun.*, 2008, 4135–4137.
34 J. H. Cavka, S. Jakobsen, U. Olsbye, N. Guillou, C. Lamberti, S. Bordiga and K. P. Lillerud, *J. Am. Chem. Soc.*, 2008, **130**, 13850–13851.
35 V. V. Rostovtsev, L. G. Green, V. V. Fokin and K. B. Sharpless, *Angew. Chem., Int. Ed.*, 2002, **41**, 2596–2599.
36 K. S. Park, Z. Ni, A. P. Côté, J. Y. Choi, R. Huang, F. J. Uribe-Romo, H. K. Chae, M. O'Keeffe and O. M. Yaghi, *Proc. Natl. Acad. Sci. U. S. A.*, 2006, **103**, 10186–10191.
37 F. Rouquerol, J. Rouquerol and K. Sing, *Adsorption by Powders and Porous Solids*, Academic Press, San Diego, 1999, pp. 204–206.
38 A. Gil, S. A. Korili and M. A. Vicente, *Catal. Rev. Sci. Eng.*, 2008, **50**, 153–221.
39 K. L. Mulfort and J. T. Hupp, *J. Am. Chem. Soc.*, 2007, **129**, 9604–9605.
40 M. Felderhoff, C. Weidenthaler, R. v. Helmolt and U. Eberle, *Phys. Chem. Chem. Phys.*, 2007, **9**, 2643–2653.
41 C. D. Wood, B. Tan, A. Trewin, H. Niu, D. Bradshaw, M. J. Rosseinsky, Y. Z. Khimyak, N. L. Campbell, R. Kirk, E. Stöckel and A. I. Cooper, *Chem. Mater.*, 2007, **19**, 2034–2048.
42 M. Oh and C. A. Mirkin, *Nature*, 2005, **438**, 651–654.
43 M. Oh and C. A. Mirkin, *Angew. Chem., Int. Ed.*, 2006, **45**, 5492–5494.
44 Y.-M. Jeon, J. Heo and C. A. Mirkin, *J. Am. Chem. Soc.*, 2007, **129**, 7480–7481.
45 Y. M. Jeon, G. S. Armatas, D. Kim, M. G. Kanatzidis and C. A. Mirkin, *Small*, 2009, **5**, 46–50.
46 A. M. Spokoyny, D. Kim, A. Sumrein and C. A. Mirkin, *Chem. Soc. Rev.*, 2009, **38**, 1218–1227.